MOLECULAR AND CELLULAR BIOLOGY, Dec. 2000, p. 9399–9408 Vol. 20, No. 24
0270-7306/00/$04.00+0

Ionophore-Resistant Mutants of *Toxoplasma gondii* Reveal Host Cell Permeabilization as an Early Event in Egress

MICHAEL W. BLACK,† GUSTAVO ARRIZABALAGA, AND JOHN C. BOOTHROYD*

Department of Microbiology and Immunology, Stanford University School of Medicine, Stanford, California 94305-5124

Received 21 June 2000/Returned for modification 24 August 2000/Accepted 20 September 2000

Toxoplasma gondii **is an obligate intracellular pathogen within the phylum Apicomplexa. Invasion and egress by this protozoan parasite are rapid events that are dependent upon parasite motility and appear to be directed by fluctuations in intracellular [Ca^{2+}]. Treatment of infected host cells with the calcium ionophore A23187 causes the parasites to undergo rapid egress in a process termed ionophore-induced egress (IIE). In contrast, when extracellular parasites are exposed to this ionophore, they quickly lose infectivity (termed ionophore-induced death [IID]). From among several Ie^- mutants described here, two were identified that differ in several attributes, most notably in their resistance to IID. The association between the Ie^- and Iid^- phenotypes is supported by the observation that two-thirds of mutants selected as Iid^- are also Ie^-. Characterization of three distinct classes of IIE and IID mutants revealed that the Ie^- phenotype is due to a defect in a parasite-dependent activity that normally causes infected host cells to be permeabilized just prior to egress. Ie^- parasites underwent rapid egress when infected cells were artificially permeabilized by a mild saponin treatment, confirming that this step is deficient in the Ie^- mutants. A model is proposed that includes host cell permeabilization as a critical part of the signaling pathway leading to parasite egress. The fact that Ie^- mutants are also defective in early stages of the lytic cycle indicates some commonality between these normal processes and IIE.**

Toxoplasma gondii is an obligate, intracellular protozoan pathogen that is capable of infecting and replicating within virtually any nucleated mammalian or avian cell. This parasite is the cause of sometimes severe disease in humans and other animals, especially those who are immunocompromised. Due to the spread of AIDS, the number of immunocompromised individuals has increased enormously with a concomitant increase in the incidence of fatal toxoplasmosis (30).

The devastating effects of uncontrolled *Toxoplasma* infections are a direct consequence of the parasite's lytic cycle. In spite of the worldwide prevalence and severity of *Toxoplasma* infections, little is known about the four general events that comprise this cycle: attachment, invasion, intracellular replication, and egress. As with many cellular events, Ca^{2+} has been shown to play a significant role in the signaling of *Toxoplasma* invasion and egress. Alterations in intracellular [Ca^{2+}] have been associated with cytoskeletal rearrangements (12), gliding motility (13), invasion (12, 16), intracellular growth (11, 19), and host cell egress (9, 23, 27). There are at least three intracellular Ca^{2+} stores in this parasite: the endoplasmic reticulum, the mitochondrion, and an unusual compartment called the acidocalcisome (14).

Among the most dramatic effects of changing [Ca^{2+}] is the egress induced by calcium ionophores (9). This ionophore-induced egress (IIE) will stimulate a population of intracellular parasites to rapidly exit their parasitophorous vacuole and thence the host cell in a manner similar to natural egress and is likely to utilize the same signaling pathway and/or secretory events. If extracellular parasites are exposed to a calcium ionophore (A23187) for prolonged periods, they irreversibly lose the ability to invade host cells (12). Since *Toxoplasma* is an obligate intracellular protozoan, the ultimate result of this inhibition is death; hence, this phenomenon is termed ionophore-induced-death (IID). Because of the wide range of activities that are regulated by [Ca^{2+}], Ca^{2+} ionophores can have dramatic effects in higher eukaryotic cells, resulting in the activation of nucleases, Ca^{2+}-dependent proteases, phosphatases, and phospholipases (6). One of the consequences of this global activation, at least in some cell lines, is the induction of apoptosis (15). In *Toxoplasma*, it is unknown whether the ionophore is directly killing the extracellular parasite or if it is merely preventing it from invading cells in some manner that is not necessarily disruptive to its metabolism.

To investigate the pathways affected by A23187, two genetic selections were developed to isolate mutants resistant to the effects of this drug. Three phenotypically distinct mutants have been recovered using this strategy that differ in their response to A23187: Ie^- Iid^-, Ie^- Iid^+, and Ie^+ Iid^-. Characterization of the events associated with IIE has also uncovered a Ca^{2+}- and parasite-dependent activity that permeabilizes both the parasitophorous vacuole and host plasma membrane as an early event, even when egress is blocked. These results were used to formulate a model for the role of Ca^{2+} in triggering egress.

MATERIALS AND METHODS

Parasite cultivation and reagents. The tachyzoite stage of the RHΔHXGPRT strain (abbreviated here as RHΔ [18, 29]) was the parent strain used here. It was maintained in vitro by serial passage on monolayers of human foreskin fibroblasts (HFF) at 37°C in 0.5% CO_2 as described previously (20). Normal medium used for propagation was Dulbecco modified Eagle medium (DMEM) (Gibco-

* Corresponding author. Mailing address: Department of Microbiology and Immunology, Fairchild Building, Room D305, 300 Pasteur Dr., Stanford University School of Medicine, Stanford, CA 94305-5124. Phone: (650) 723-7984. Fax: (650) 723-6853. E-mail: john.boothroyd@stanford.edu.

† Present address: Medical Research Council, Laboratory of Molecular Biology, Cambridge CB2 2QH, United Kingdom.

BRL) supplemented with 10% NuSerum (Collaborative Biomedical Products), 2 mM glutamine, and 20 μg of gentamicin/ml. Parasites were transformed by electroporation as previously described (26). Drug selection was not initiated until after overnight growth on a monolayer of HFF in normal medium. Plaques were scored after 5 to 6 days of growth by fixing the monolayer with 100% methanol and staining it with either Giemsa stain or crystal violet (20).

Mutagenesis was performed using a monolayer of HFF in a T175 flask (Falcon) that was heavily infected with *Toxoplasma* at a multiplicity of infection (MOI) of ~5 and was allowed to grow for 30 h in normal growth medium. The mutagen *N*-nitroso *N*-ethylurea (ENU; Sigma) was added to this monolayer at 150 μM in normal growth medium and was allowed to incubate at 37°C for 60 min. After three washes, the cells were scraped off the flask and the parasites were syringe released using a 27-gauge needle followed by replating on a fresh monolayer for propagation. The typical mutagenesis using 150 μM ENU resulted in ~65% survival after treatment compared to that for the unmutagenized control, resulting in 2×10^7 to 4×10^7 mutagenized parasites/T175 flask. Parasites surviving the mutagenesis were passed a second time without selection and were tested for survival under 5-fluorodeoxyuridine selection to gauge the efficiency of mutagenesis (17). Typically, ~200 parasites per million were resistant to this drug, presumably due to mutations in the uracil phosphoribosyltransferase gene (8). Control cultures showed $<10^{-6}$ resistant parasites, confirming that the ENU mutagenesis had been successful.

The calcium ionophore A23187 (Sigma) was dissolved in dimethyl sulfoxide (DMSO) at 1 mM. Hanks balanced salts solution (HBSS; Gibco-BRL) was modified for use in two different forms: (i) $HBSS_c$ with 1 mM $MgCl_2$, 1 mM $CaCl_2$, 10 mM $NaHCO_3$, and 20 mM HEPES, pH 7.2; and (ii) $HBSS_{nc}$, which is $HBSS_c$ with 5 mM EGTA and no added $CaCl_2$. Cytochalasin D (Sigma) was dissolved in DMSO at a concentration of 1 mM. The cell-permeable calcium chelator BAPTA-AM (Sigma) was dissolved in DMSO at 50 mM.

Quantitation of IIE phenotype. An HFF monolayer was grown on 24-well plates and infected with *Toxoplasma* at an MOI of 0.2 parasites/fibroblast. Parasites were allowed to replicate for 30 to 36 h at 37°C to develop vacuoles that contained 32 to 64 parasites. The growth medium was washed off the monolayer with phosphate-buffered saline (PBS) and replaced with warm HBSSc containing 1 μM A23187 for time points ranging from 0 to 10 min. Upon removal of the ionophore, monolayers were fixed with 100% methanol and stained with crystal violet as described previously (20). Vacuoles were examined by light microscopy to determine if egress had occurred by counting no fewer than five fields from each well (≥150 vacuoles) at a magnification of ×200. Intact vacuoles versus those where egress had occurred were readily distinguished by the tight clustering of parasites within a discrete vacuole versus a group of widely dispersed individual parasites around a lysed host cell.

Selection for Iie$^-$ mutants. The RHΔ strain was chemically mutagenized and passaged once without selection. The lysing mutant population from T175 was syringed with a 27-gauge needle and seeded onto a fibroblast monolayer at an MOI of 1 parasite/fibroblast. Thirty to thirty-six hours after infection (32 to 64 parasites/vacuole), the growth medium was removed and the cultures were washed with PBS followed by incubation in warm $HBSS_c$ containing 1 μM A23187 for 2 min at 37°C. Most extracellular parasites were immediately washed off with cold PBS, and the entire surface of the monolayer (including remaining extracellular and attached parasites) was biotinylated for 30 min at 4°C with $HBSS_c$ containing 0.25 mg of NHS-biotin (Pierce)/ml. The infected monolayer was washed three times with PBS containing 1% bovine serum albumin (BSA), scraped off the flask, and passed through a syringe with a 27-gauge needle to release the intracellular, unbiotinylated parasites from the host cells. The cell debris was pelleted at $500 \times g$ for 5 min and discarded. Parasites in the supernatant were pelleted at $1{,}000 \times g$ for 10 min and resuspended in 0.5 ml of $HBSS_c$ and mixed (1:1) with streptavidin-conjugated Sepharose beads (Sigma). A column was constructed by adding the slurry to a polyfill-plugged Pasteur pipette. The flowthrough was passed over the column three times and followed by 10 column volumes of DMEM containing 10% fetal bovine serum (FBS) to wash off the biotin-free parasites. The final flowthrough fraction, enriched for unbiotinylated parasites (i.e., parasites that were intracellular during the biotinylation step), was added to a fresh HFF monolayer for subsequent rounds of growth and selection.

A secondary selection was performed to eliminate parasites that exit the cell normally upon ionophore treatment but rapidly invade neighboring cells. After five rounds of selection, the population was seeded onto monolayers in 100-mm tissue culture dishes (Falcon) at an MOI of 0.05 parasite/fibroblast and was incubated for 30 to 36 h (~32-cell stage). Egress was induced with A23187 as described above for 2 min followed by two washes with PBS and addition of medium with 0.9% molten Bacto-Agar as previously described (20). Full vacuoles were picked using a Pasteur pipette and were transferred to HFF monolayers in a 96-well plate. Single PFU were chosen and labeled as MBEx.y, where "E" indicates an egress mutant, "x" represents the experiment number, and "y" is the clone number in that experiment. Thus, for example, MBE1.1 and MBE2.1 are egress mutants that underwent completely independent rounds of mutagenesis and selection.

Quantitation of IID phenotype. Parasites were syringe released from lysing monolayers of infected HFF, and the host cell debris was pelleted at $500 \times g$ for 5 min. Extracellular parasites were pelleted from the supernatant at $1{,}000 \times g$ for 10 min and were resuspended at a concentration of 10^5 parasites/ml in 37°C $HBSS_c$ containing 1 μM A23187 in DMSO or a comparable amount of DMSO alone. This suspension was incubated at 37°C for time points ranging from 0 to 60 minutes. At specified times, samples were taken and plated onto monolayers in 24-well plates for plaque development. After 5 or 6 days, the plates were fixed with 100% methanol and stained with crystal violet to score the number of PFU as a function of time of incubation in the ionophore.

Selection for Iid$^-$ mutants. The RHΔ strain was chemically mutagenized and passaged once without selection as described above. The mutagenized population from a T175 flask was syringed with a 27-gauge needle and pelleted at $1{,}000 \times g$ for 10 min. The parasites were resuspended in warm $HBSS_c$ that contained 1 μM A23187 and were incubated for 30 min at 37°C followed by pelleting for 10 min at $1{,}000 \times g$. The entire pellet of parasites was resuspended in DMEM plus 10% FBS and plated onto a fresh HFF monolayer in a T75 flask. Following expansion of this population, a second round of selection was performed in which the extracellular parasites were incubated in A23187 for 45 min instead of 30 min at 37°C. Parasites recovered from the pellet were plated onto a T25 flask for rounds 3 to 5 using 45-, 50-, and 60-min incubations, respectively. The population that survived round 5 was plated onto monolayers in a 96-well plate at a limiting dilution (2 to 6 parasites/well) for isolating clones. Twelve clones were isolated from each of two independent populations of mutagenized parasites for a total of 24 clones that were analyzed further.

Ionophore-induced MIC2 secretion. This protocol was obtained from V. Carruthers and D. Sibley at Washington University, St. Louis, Mo. (3). Parasites were syringe released using a 27-gauge needle from a lysing HFF monolayer in a T25 flask. After two washes with invasion medium (DMEM with 3% FBS, 0.04% $NaHCO_3$, 2 mM glutamine, and 20 mM HEPES, pH 7.2), parasites were resuspended in the same medium at 5×10^7 cells/ml. A 96-well round-bottom plate (Falcon) was prepared with 1 μl of either DMSO or 10 μM A23187 in DMSO in each of 3 wells with 3 additional wells left empty. The plate was transferred to a 37°C bath, and 100 μl of the parasite suspension was added to each well. After 2 min, the suspensions containing DMSO or A23187 in DMSO were transferred to a new plate on ice, leaving the third set of wells at 37°C for a total of 30 min (basal secretion). The suspensions were then cleared by pelleting the cells at $1{,}000 \times g$ for 5 min at 4°C, and 70-μl samples of the supernatant were transferred to a new plate. These samples were respun using the same parameters, and 30-μl samples of the resulting supernatants were taken for sodium dodecyl sulfate-polyacrylamide gel electrophoresis and Western blot analysis as described before (1). Nitrocellulose filters were stained with the monoclonal anti-MIC2 antibody 6D10 (29) (a generous gift of D. Sibley) and a secondary peroxidase-conjugated goat anti-mouse antibody and were then analyzed using ECL fluorescent detection reagents (Amersham).

Invasion rate assay. Intracellular parasites grown for approximately 48 h at 37°C were syringe released. These parasites were added to HFF cells in 12-well plates at an MOI of 0.1. The plates were then incubated at 37°C for 24 h to allow invasion. At this point the medium was removed, the monolayer was washed twice with PBS, and fresh medium was added. The plates were then incubated at 37°C for an additional 4 days to allow the formation of plaques.

Immunofluorescence analyses. Gliding motility was assessed indirectly by immunofluorescence analysis of the major *Toxoplasma* surface antigen SAG1 in trails (7). Parasites were immobilized in K_2SO_4 buffer (44.7 mM K_2SO_4, 106 mM sucrose, 10 mM $MgSO_4$, 20 mM Tris-H_2SO_4 [pH 8.2], 5 mM glucose, and 3.5 mg of BSA/ml [10]) and were seeded onto a tissue culture-treated LabTek chamber slide. After 15 min at 37°C, the K_2SO_4 buffer was removed and replaced with either the same medium or $HBSS_c$ and the parasites were incubated for 2 min more at 37°C. The parasites were then fixed with 3% formaldehyde for 20 min at room temperature and stained using the anti-SAG1 monoclonal antibody (MAb) DG52 (2), used at 1/1,000, followed by fluorescein isothiocyanate (FITC)-conjugated goat anti-mouse immunoglobulin G secondary antibody (ICN), used at 1/1,000. Chambers were removed, and coverslips were mounted on slides with Vectashield (Vector Laboratories) and examined using an Olympus BX60 fluorescence microscope (also used in each of the following protocols).

The integrity of host plasma and vacuolar membranes was examined by using immunofluorescence and differential permeabilization. Monolayers of HFF were grown on HCl-ethanol-etched round glass coverslips and were infected with parasites at an MOI of 0.2 parasites/fibroblast. Thirty hours postinfection, the medium was removed, washed off with PBS, and replaced with $HBSS_c$ containing 1 μg of cytochalasin D/ml for 5 min at 37°C to immobilize the intracellular parasites. An equal volume of $HBSS_c$ containing 2 μM A23187 (for final concentrations of 1 μM A23187 and 0.5 μg of cytochalasin D/ml) was added to the medium for 2 min before fixing the cells with 3% formaldehyde in PBS. A rabbit anti-SAG1 polyclonal serum (RαP30, a generous gift of L. Kasper, Dartmouth University), detected with an FITC-conjugated secondary antibody, was used to stain parasites that were extracellular or within disrupted host cells. A mouse anti-SAG1 monoclonal cell line (DG52 [2]) was used in the presence of Triton X-100 and was detected with a Texas red-conjugated secondary antibody to stain all the parasites regardless of the state of their host cell.

^{51}Cr-release assay. A 24-well plate of *Toxoplasma*-infected HFF (24 h postinfection at an MOI of 0.2) was loaded with ^{51}Cr at 10 μCi/5×10^5 fibroblasts in 0.3 ml of DMEM plus 10% FBS per well. After 12 h at 37°C, the monolayer was washed five times with PBS and then incubated in PBS containing either 50 μM BAPTA-AM (Sigma) in DMSO or DMSO alone for 30 min at 37°C. The wells were washed once with PBS and treated with 0.5 ml of $HBSS_c$ containing either

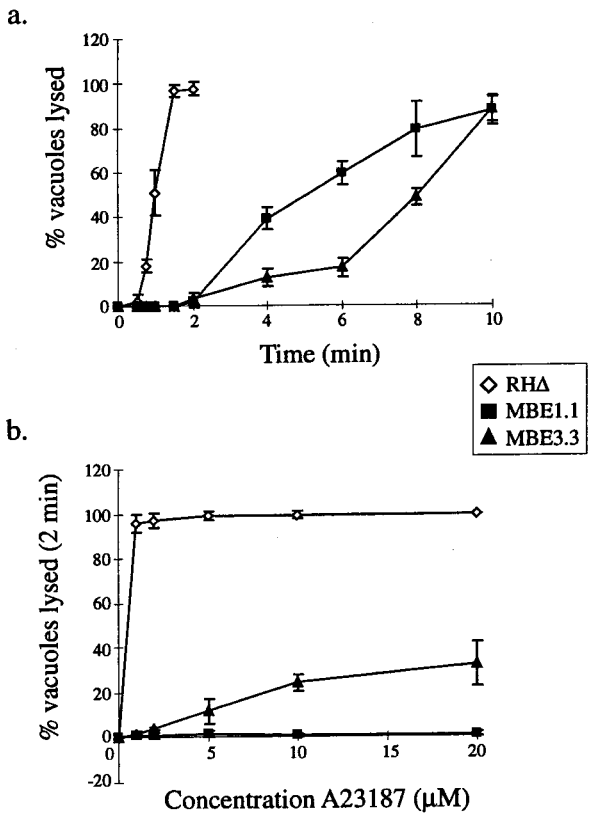

FIG. 1. The IIE phenotype of wild-type (RHΔ) and two Iie$^-$ mutants (MBE1.1 and MBE3.3). (a) A time course of egress using 1 μM A23187 in $HBSS_c$. (b) IIE as a function of A23187 concentration. Egress was measured after 2 min of exposure to the ionophore. Monolayers for both panels a and b were scored for the percentage of lysed vacuoles per field.

1 μg of cytochalasin D/ml in DMSO or DMSO alone for 5 min at 37°C. At the end of this incubation, 50 μl of the culture supernatant was taken for the 0-min time point and replaced with 50 μl of $HBSS_c$ containing 50 mM dithiothreitol (DTT), 5 μM A23187 in DMSO, or DMSO alone. Ten percent of the total remaining volume (30 to 50 μl) was transferred to 96-well scintillation plates (Wallac) containing 150 μl of optiphase polysafe scintillation fluid (Wallac) at time points from 2 to 10 min. After taking the 10-min time point, each well was lysed with Triton X-100 (1% final concentration), and 10% of the supernatant was taken to determine the total remaining counts per well. The 96-well plates were sealed and analyzed using a 1450 Microbeta Plus counter (Wallac). The data obtained were normalized to 10^4 PFU as determined by a parallel plaque assay that was performed on each strain. Egress assays for both A23187 (1 μM) and DTT (10 mM) were also performed in parallel plates as described above.

Saponin permeabilization of the host cell plasma membrane. HFF monolayers in 24-well plates were infected with mutant or parental parasite strains at an MOI of 0.2. After 30 h of growth (~32-cell stage), the host plasma membrane was permeabilized using 0.005% saponin (Sigma) in $HBSS_c$ or $HBSS_{nc}$ ($HBSS_c$ with 5 mM EGTA and no added $CaCl_2$) for 20 min at 4°C. Plates were immediately placed in a 37°C water bath in the same solution and fixed with 100% methanol at time points ranging from 0 to 5 min after the temperature shift. Monolayers were stained and assayed to determine the percent egress as described above.

RESULTS

Isolation of ionophore-induced egress mutants. To devise a selection strategy for the isolation of IIE-defective (Iie$^-$) mutants, it was first necessary to determine the kinetics of A23187-induced egress from infected host cells using the RHΔ parental strain. These studies showed that >98% of the parasite population will exit from their vacuoles and hence their host cells after only a 2-min exposure to 1 μM A23187 (Fig. 1a). This event is temperature dependent, as the frequency of egress decreased with lower temperatures and can be completely blocked at 4°C (data not shown).

TABLE 1. Phenotypes of three A23187-resistant mutants compared to the parental strain[a]

Phenotype	RHΔ	MBE1.1	MBE3.3	MBD2.1
Ionophore-induced egress	+	−	−	+
Ionophore-induced death	+	−	+	−
Efficient invasion	+	−	−	+
Ionophore-induced permeabilization	+	−	−	+
Saponin-induced egress	+	+	+	+
BAPTA insensitivity	+	+	+	−
Conoid extrusion				
Intracellular	ND	+	−	ND
Extracellular	+	+	+	+
Induced microneme secretion	+	+	+	ND
Gliding motility	+	+	+	ND

[a] ND, not determined.

The selection strategy for isolating Iie$^-$ mutants was performed using a chemically mutagenized population of RHΔ to infect an HFF monolayer. Briefly, 1 μM A23187 was added to infected cultures at 37°C for 2 min to allow IIE-responsive parasites to leave the host, many of which were immediately washed off. However, because many of the extracellular parasites remain adherent to the monolayer, NHS-biotin was used to tag and differentiate the extracellular parasites. The monolayer was washed with PBS to remove the residual biotin and was scraped from the flask, and the parasites still within the cells were syringe released. Biotinylated parasites were removed by passing them over a streptavidin-Sepharose column. Unbiotinylated parasites were washed through the column and recovered in normal medium for propagation on a fresh HFF monolayer. This population, now enriched for Iie$^-$ mutants, was passed through four more complete rounds of the selection, as detailed in Materials and Methods.

The efficiency of the selection was compromised by the fact that many of the ionophore-responsive parasites immediately invade neighboring cells after exiting the original host cell. To overcome this limitation of the selection, a secondary screen was performed to separate the Iie$^-$ mutants from the background of wild type. After ionophore treatment, full vacuoles containing presumptive mutants were identified by phase microscopy and individually picked using a plugged Pasteur pipette. Through this final selection, a total of five Iie$^-$ mutants were isolated and cloned from three independent mutagenesis/selection experiments. Three clones isolated from three separate mutant populations have been examined in detail, with two (MBE1.1 and MBE2.1) showing indistinguishable phenotypes. Thus, the results for only one of these two (MBE1.1) and the third mutant, MBE3.3, which has a distinct phenotype, are presented in this report.

As expected, MBE1.1 and MBE3.3 demonstrate a dramatic shift in the timing of host exit, with <5% of the vacuoles responding after a 2-min exposure to ionophore as compared to >95% in the parental strain (Fig. 1a; this and the other phenotypes described below are summarized in Table 1). With longer incubations, however, the mutants do eventually respond, such that by 10 min ~90% have exited their host cells.

The 2-min time point was used to titrate the response to ionophore at concentrations ranging from 1 to 20 μM. As shown in Fig. 1b, MBE1.1 did not show any significant change in its phenotype at even the highest concentration of the ionophore, which is 20 times that used for the selection. MBE3.3, however, appeared to be more responsive as the concentration

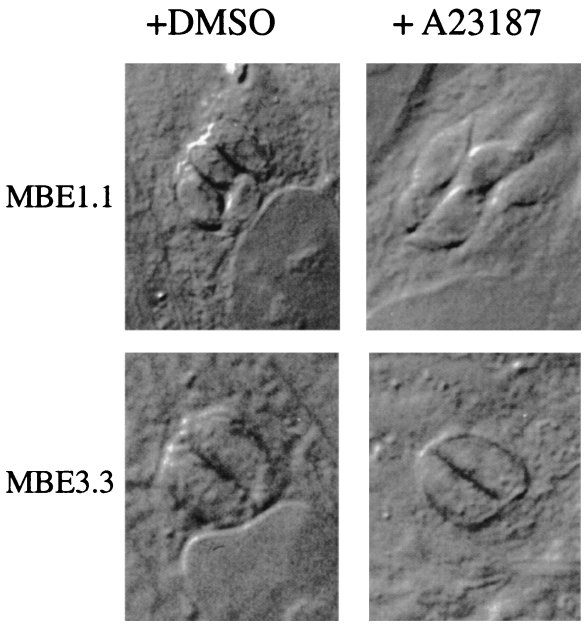

FIG. 2. A23187 induction of parasite elongation in intracellular Iie$^-$ mutants. Infected cells were treated with DMSO (left) or 1 μM A23187 (right) in $HBSS_c$ and were fixed after 2 min at 37°C. The morphological phenotype is observed as an extension of the apical end (pointing out from the center of the vacuoles). Intracellular MBE1.1 parasites demonstrate this phenotype, while those of the MBE3.3 strain remain rounded.

of ionophore was elevated, with ~30% leaving their vacuole at 20 μM. The difference in sensitivity to elevated concentrations of A23187 suggests that these mutants are distinct in their mechanism of resistance to IIE.

Cytoskeletal rearrangements associated with A23187 exposure. The mutations that prevent MBE1.1 and MBE3.3 from rapidly exiting in response to ionophore induction may be at either of two levels: the mutants either could be incapable of receiving and transducing the signal that is stimulated by the rise in intracellular [Ca^{2+}] or could be able to receive the signal but be incapable of reacting to it at points downstream in the response pathway (e.g., no longer able to initiate motility).

To discriminate between these two scenarios, the phenotypes of the two mutants were examined under various conditions related to the ionophore-induced egress. First, it has been observed that upon exposure to A23187, extracellular parasites will extrude their conoid, a cytoskeletal appendage localized to the anterior pole (12). Although extracellular [Ca^{2+}] does not appear to play a significant role in this event, it is dependent upon intracellular [Ca^{2+}] and can be completely blocked by the cell-permeable calcium chelator BAPTA-AM (12). Extracellular parasites from the RHΔ, MBE1.1, and MBE3.3 strains were treated with concentrations of A23187 ranging from 0.1 to 1 μM in $HBSS_c$ for 2 min at 37°C. In none of the conditions tested was there any observable difference between the parental and Iie$^-$ mutants, with 75% or more of the parasites extruding their conoids at 1 μM (data not shown).

Next, the effect of the ionophore on conoid extrusion in intracellular parasites was examined. As shown in Fig. 2, MBE1.1 parasites that remain intracellular after a 2-min exposure to A23187 undergo a noticeable morphological alteration that appears to elongate the parasite and extend the conoid, similar to what is observed in extracellular forms. This form of movement resembles the twisting and torsional movements previously described in extracellular parasites during the invasion event (5). Although this has been difficult to observe in the parental strain due to the rapid IIE response, video analysis has suggested that a similar cytoskeletal rearrangement occurs in RHΔ just prior to the onset of motility (data not shown). In MBE3.3, however, this morphological change was not seen; the intracellular parasites showed no elongation or conoid protrusion after the 2-min incubation (Fig. 2). As observed in the conoid extrusion by extracellular parasites, the cytoskeletal rearrangement in MBE1.1 is completely inhibited if the infected cells are first loaded with 50 μM BAPTA-AM for 30 min (data not shown), indicating a dependence on [Ca^{2+}].

Gliding motility is not disrupted in Iie$^-$ mutants. To further investigate the nature of the defect in the mutants, gliding motility was examined in the two strains independent of the influence of A23187 by immunofluorescence analysis of deposited surface protein trails (7). There was no apparent difference in the length or number of protein trails deposited between the mutants and the parental strain using this assay (data not shown). This is consistent with visual observations of naturally lysing cultures: there was no observable difference in the motility of the mutants compared with the parental strain. These results suggest that the Iie$^-$ phenotype in the mutant strains is not due to a defect in the general motility apparatus required for gliding.

IID phenotype in Iie$^-$ mutants. As mentioned before, A23187 will irreversibly block the ability of extracellular parasites to invade host cells after prolonged exposure, causing IID (12). To investigate the relationship between the Iie$^-$ phenotype and IID, MBE1.1 and MBE3.3 were tested as described in Materials and Methods for their ability to resist prolonged exposure to ionophore. As shown in Fig. 3a, the efficiency of plating (EOP) of both RHΔ and MBE3.3 dropped to 10% of that obtained for the DMSO controls after only a 30-min exposure to A23187. By 45 min, both strains were below the detection limit of the assay. The MBE1.1 strain, however, was barely affected by the ionophore, so that even after a 60-min exposure the EOP was approximately 70% of that obtained for the DMSO control.

Ionophore-induced microneme secretion appears normal in the Iie$^-$ mutants. It has been recently observed that extracellular forms of *Toxoplasma* can be induced to secrete micronemal contents, specifically the MIC2 protein, upon exposure to A23187 (3). As this protein is homologous to a family of proteins in *Plasmodium* that are essential for motility and invasion (28, 29), the premature exhaustion of micronemal contents could be a contributing factor to both IIE and IID. This would predict that a delay in their secretion would both hinder the onset of induced egress and allow extracellular parasites to survive for longer periods in the presence of A23187.

MIC2 is a 115-kDa protein that is secreted onto the surface of the parasite and is anchored in the plasmalemma via a transmembrane domain. Smaller, soluble forms of this protein (96 kDa) can be isolated from the media and are believed to be the products of a proteolytic event, leaving the transmembrane portion on the surface of the parasite (29). In a collaboration with V. Carruthers and D. Sibley (Washington University, St. Louis, Mo.), ionophore-induced secretion was examined in the RHΔ, MBE1.1, and MBE3.3 strains, using the release of the soluble fragments as an assay. Phospho-imaging analysis of MIC2 showed no significant difference in the levels of secretion between the parental and Iie$^-$ strains (data not shown). Although this does not eliminate the possibility that induced secretion from the micronemes plays a role in IID, it is unlikely that a defect in this process is responsible for the Iid$^-$ pheno-

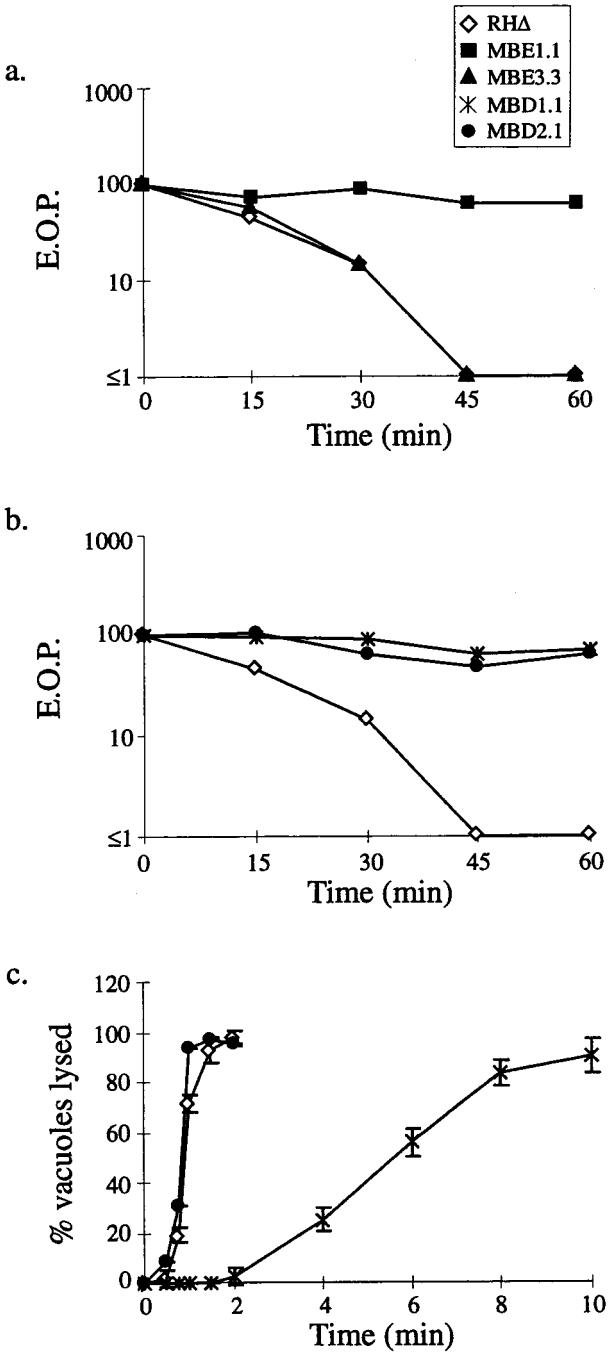

FIG. 3. Relationship between the IIE and IID phenotypes. (a) MBE1.1, but not MBE3.3, is resistant to IID. Extracellular parasites were exposed to A23187 and assayed for the formation of plaques. EOP was defined as the percentage of the PFU arising from parasites incubated with A23187 versus the DMSO-treated control. (b) Iid$^-$ phenotypes of MBD1.1 and MBD2.1, two independent mutants isolated in the Iid$^-$ selection. Assays were performed as in panel a. (c) IIE in the Iid$^-$ selected mutants. MBD1.1 is Iie$^-$, while MBD2.1 is Iie$^+$. The IIE assay was performed as described for Fig. 1a.

type of MBE1.1 or the Iie$^-$ phenotype of MBE1.1 and MBE3.3.

Isolation of IID mutants. The double defect in MBE1.1 (Iie$^-$ and Iid$^-$) could be due to a single, pleiotropic mutation or to two independent mutations. To investigate further the association between IIE and IID, a genetic selection was employed to isolate mutants in the RHΔ strain that are Iid$^-$ and which could then be screened for an associated Iie$^-$ phenotype. The selection strategy was to expose an extracellular population of chemically mutagenized parasites to 1 μM A23187 for prolonged periods (30 to 60 min) before allowing them to infect fibroblast monolayers and then recovering the survivors. After five rounds of this selection, the surviving parasites were plated at a limiting dilution to isolate clones. The Iid$^-$ phenotype of a representative clone from each of two independent mutagenesis and selection experiments, MBD1.1 and MBD2.1, is shown in Fig. 3b. Both strains showed a nearly complete resistance to the IID effect, such that by 60 min there was little if any drop in infectivity in the mutants compared with a complete loss of viability in the parental strain.

Next, 24 Iid$^-$ clones (12 from each of two independently mutagenized and selected populations) were examined for their IIE phenotype. The results for two representative clones are shown in Fig. 3c. Following a 2-min exposure to 1 μM A23187, MBD1.1 demonstrated a delay in IIE similar to that observed for MBE1.1 and MBE3.3 (less than 5% of the vacuoles lysing after 2 min), while MBD2.1 behaved as the wild type in this assay. Thus, MBD2.1 represents a new class of mutant that has an Iie$^+$ Iid$^-$ phenotype. Of the 24 Iid$^-$ mutants characterized, 16 (8 from each of the two independently mutagenized populations) were Iid$^-$ Iie$^-$, indicating an association between these two phenotypes and strongly suggesting that a single mutation can give rise to both phenotypes.

IID is not due to a freely diffusible, toxic product. An alternative to the exhaustion model for the IID effect is that the stimulated parasites release a toxic substance. To test this possibility, the three classes of A23187-resistant mutants (represented by MBE1.1, MBE3.3, and MBD2.1) and the parental RHΔ were mixed with an RHΔ-βgal strain (24) and examined for "trans" killing. Since expression of the *lacZ* (βgal) gene does not affect the IID phenotype of the parental RHΔ (data not shown), this strain was used to differentiate the blue Iid$^+$ wild-type strain from the colorless mutant strains. As shown in Fig. 4, the IID of RHΔ-βgal parasites (Fig. 4a) did not substantially affect the viability of MBE1.1 or MBD2.1 (Fig. 4b) compared to experiments where the wild-type parasites were not included (Fig. 3). Thus, the effect of A23187 on the EOP of Iid$^+$ strains is not due to the secretion of a large amount of a stable and readily diffusible toxic factor. The results do not, however, exclude the possibility that a toxic factor is released but can only act locally on the parasite that releases it.

MBD2.1 mutant is hypersensitive to BAPTA-AM. The roles of intracellular [Ca^{2+}] in *Toxoplasma* motility and invasion have been well documented using a variety of assays. For example, it has been observed that effectively removing the calcium stores in extracellular parasites by pretreating with BAPTA-AM results in a >90% reduction in the ability of the parasite to invade host cells (12). Since the IID phenotype exhibits a similar effect, the sensitivity of the Iie$^-$ and Iid$^-$ mutants to BAPTA-AM treatment was examined. Extracellular parasites of the MBE1.1, MBE3.3, MBD2.1, and RHΔ strains were treated with either 50 μM BAPTA-AM in DMSO or an equivalent concentration of DMSO alone in $HBSS_c$ for 30 min at 37°C. After pretreatment, the parasites were diluted and plated onto fresh, untreated HFF monolayers for the development of plaques (Fig. 5). Like RHΔ, the MBE1.1 and MBE3.3 mutants showed an approximately 90% drop in their EOP. In contrast, the MBD2.1 mutant appears to be hypersensitive to BAPTA-AM, showing a 99% drop in its EOP. This result suggests that the Iid$^-$ phenotype of MBD2.1 may be due to a diminished ability to respond to elevated intracellular

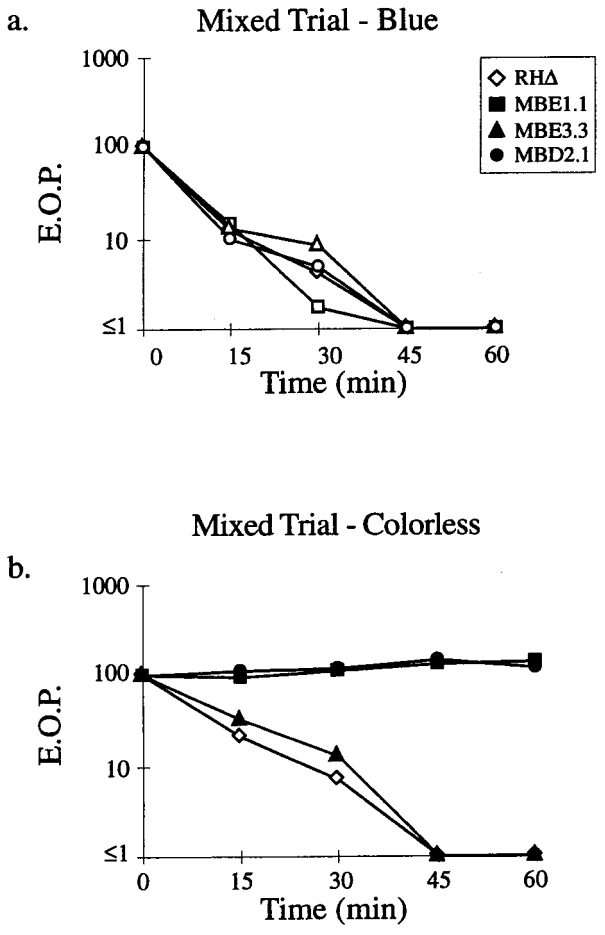

FIG. 4. IID is not due to a freely diffusible lytic activity. A strain of RHΔ that was transformed with a SAG1-driven β-galactosidase reporter (24; RHΔ-βgal) was used as the Iid$^+$ strain and mixed with RHΔ, MBE1.1, MBE3.3, or MBD2.1 in a 1:1 ratio. The extracellular parasites were incubated in 1 μM A23187 in $HBSS_c$ at 37°C for periods of 0 to 60 min, diluted, and plated on HFF monolayers for the development of plaques. After 5 days, the monolayers were fixed and stained with 5-bromo-4-chloro-3-indolyl-β-D-galactopyranoside (X-Gal) to distinguish the plaques from each strain. After counting the blue plaques, the monolayer was counterstained with crystal violet to score all the remaining "colorless" plaques. (a) Control showing the expected drop in EOP of the Iid$^+$ RHΔ-βgal strain in the four coincubation assays from panel b (scoring for blue plaques). (b) The effect of coincubation with RHΔ-βgal on the IID phenotype of the four strains.

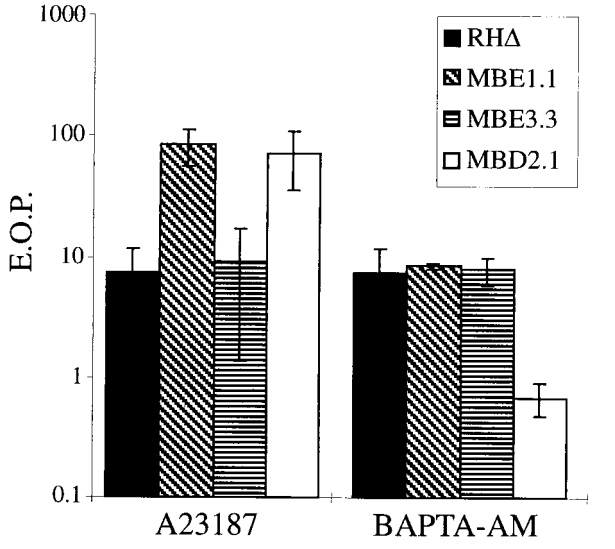

FIG. 5. The effect on EOP of pretreating extracellular parasites with either A23187 or BAPTA-AM. Extracellular parasites were pretreated with either 1 μM A23187 or 50 μM BAPTA-AM in $HBSS_c$ for 30 min at 37°C and were plated to determine the EOP expressed as the percent relative to treatment with DMSO alone. The data are pooled from three independent trials. The two Iid$^+$ strains (RHΔ and MBE3.3) showed the expected drop in EOP after exposure to A23187. Upon treatment with BAPTA-AM, RHΔ, MBE1.1, and MBE3.3 showed about a 90% drop in EOP while MBD2.1 was hypersensitive to this treatment, with a drop of over 99%.

[Ca^{2+}]. Since MBD2.1 is Iie$^+$, the mutation it harbors is likely to create a defect that is distinct from that which makes MBE1.1 Iie$^-$ Iid$^-$.

IIE mutants exhibit reduced EOP. Because several events detected during IIE, such as conoid protrusion and [Ca^{+2}] flux, are also part of the invasion process, it seems likely that these two processes are related. Therefore, we tested whether the Iie$^-$ mutants have a defect in invasion by looking at their EOP. Mutant and parental parasites were syringe released and allowed to invade new cells for 24 h. Noninvaders were removed by extensive washing, and the plates were incubated for 3 more days to allow the formation of plaques. All three Iie$^-$ mutants formed ~30 to 50% fewer plaques than the wild type, whereas the Iie$^+$ Iid$^-$ mutant MBD2.1 showed no such decrease (Fig. 6). The EOP reduction was independent of the length of time the parasites were given to invade, which was over a range from 0.5 to 24 h (data not shown). The decrease was not due to a general growth defect because no difference from wild type was seen for any of the mutants when the number of parasites per vacuole was counted as a function of time (data not shown). Thus, regardless of the selection method, the mutants displaying an egress phenotype were also defective in invasion and/or the earliest stages of intracellular growth (our data do not discriminate between failure to invade and failure to survive

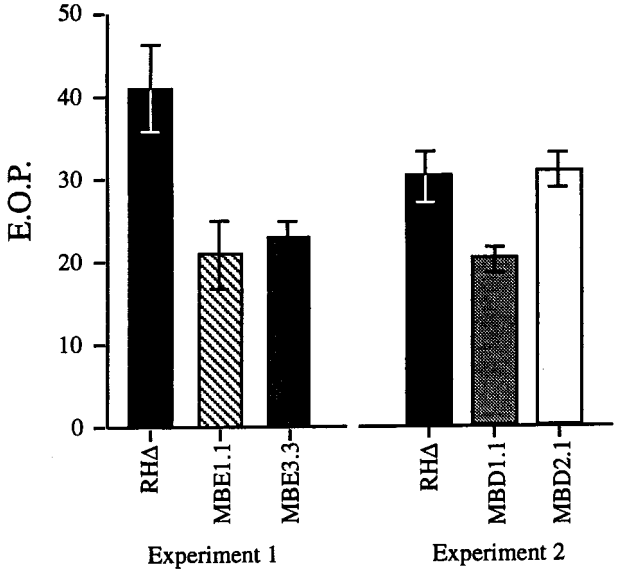

FIG. 6. EOP of Iie$^-$ and Iid$^-$ mutants. Parasites were allowed to infect HFF monolayers for 24 h, after which extracellular parasites were removed and the plaques were allowed to develop for 4 more days. Mutants defective in IIE also showed a reduction in the efficiency of plaquing.

once inside). These results show that the mutated genes are involved in the normal functioning of the parasite, not just in IIE, and establish a connection between the IIE phenomenon and the initial stages of the lytic cycle.

Host cell permeabilization is an early event in IIE. The effect of A23187 treatment on infected host cells, apart from the ultimate disruption of the cell from parasite egress, was examined using cytochalasin D to immobilize intracellular forms of the RHΔ strain. Cytochalasin D is a microfilament-depolymerizing agent that reversibly inhibits both conoid extrusion (12) and gliding motility (7, 21, 25). In preliminary experiments using video microscopy, it was observed that when cultures were pretreated with cytochalasin D and then exposed to 1 μM A23187 at 37°C, the infected host cells initially swelled and then apparently collapsed down around the parasites and host cell nucleus as though grossly permeabilized (data not shown). During this lysis neither host cell organelles nor parasites were released. The lysis was seen only in infected cells; adjacent, uninfected cells showed no signs of any perturbation.

To visualize this phenomenon and obtain quantitative data, two assays were used. The first was an examination of the permeability of the host cell membrane by using antibodies directed to the parasite; only if the host plasma membrane and the parasitophorous vacuolar membrane are severely permeabilized should antibody be able to reach the parasite. The latter is normally permeable only to molecules below 1.4 kDa (23), well below the size of an antibody. To do this assay, infected monolayers that had been treated with cytochalasin D and then ionophore were fixed and stained with a rabbit polyclonal antibody to a parasite surface antigen, SAG1. The monolayers were then permeabilized with detergent and stained with a mouse MAb to SAG1 to allow all parasites to be identified regardless of the state of the host membranes. In cultures infected with wild-type parasites, the ionophore-induced but paralyzed intracellular parasites stained with both antibodies, indicating severe permeabilization of the infected host cells (Fig. 7a). This effect is Ca^{2+} dependent, because pretreatment with BAPTA-AM blocked ionophore-induced permeabilization (Fig. 7b). Since BAPTA-AM also blocks IIE (data not shown), ionophore-induced permeabilization and IIE may both be consequences of elevated $[Ca^{2+}]$ inside the host cell and/or parasite. Nevertheless, BAPTA-AM would not be expected to enter the parasite in this experiment, because it should be deesterified by the host cell and thus be unable to cross the parasite's plasma membrane (27).

The association between host lysis and IIE was examined further using the three mutant strains. As shown in Fig. 7a, a clear difference in the permeabilization response in the presence of cytochalasin D was observed between the Iie^- mutants (MBE1.1 and MBE3.3) and the mutant with an Iie^+ phenotype (MBD2.1) following a 2-min exposure to ionophore. Thus, IIE appears to be associated with permeabilization of host membranes. The lack of permeabilization of cells infected with Iie^- mutants also shows that neither the cytochalasin D nor the ionophore itself is directly responsible for the permeabilization.

To quantitate the timing of host lysis and the differences between the wild-type and mutant strains, a chromium-release assay was performed on infected host cells preloaded with [^{51}Cr]. In addition, IIE assays were performed in parallel so that the number of vacuoles lysed could be compared to the level of ^{51}Cr release. As shown in Fig. 8a and b, the timing of ionophore-induced ^{51}Cr release in RHΔ-infected monolayers pretreated with cytochalasin D parallels that observed in the absence of cytochalasin D. Although the IIE response in this experiment was similar to that in previous assays (>98% egress

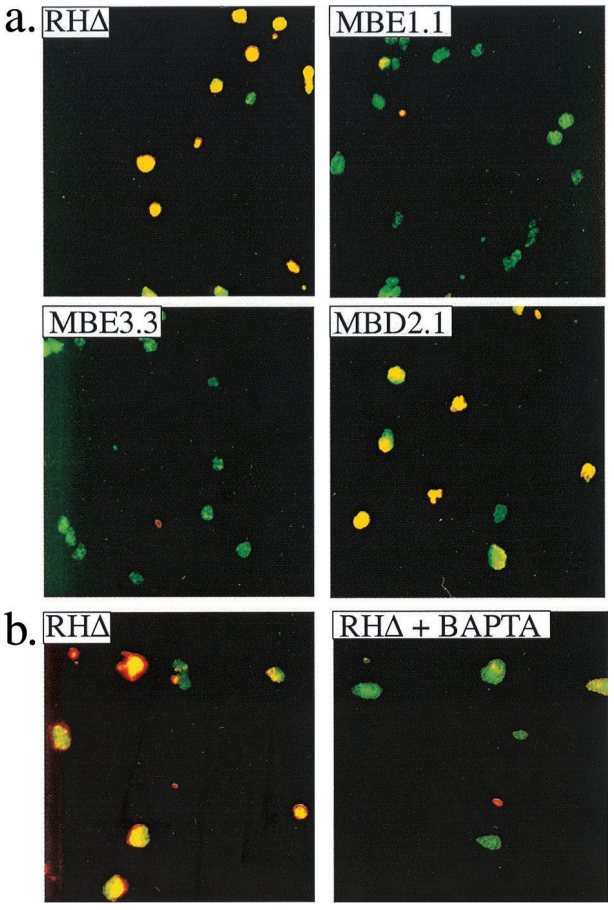

FIG. 7. Ionophore-induced membrane permeabilization by intracellular Iie^+ parasites. Infected cells were pretreated with cytochalasin D to block parasite motility, and A23187 was added before fixing the monolayer. Immunofluorescence was used to examine the membrane integrity of host cells infected with Iie^+ and Iie^- strains. A rabbit anti-SAG1 antibody was used before permeabilizing the monolayer with detergent so as to stain all the parasites that are extracellular or within permeabilized host cells. A mouse anti-SAG1 MAb was used in the presence of Triton X-100 to permeabilize all membranes and allow all the parasites to be stained regardless of their location or the state of the host cell. The two antibodies were detected with different fluorescent dyes, rabbit antibodies with Texas red and mouse antibodies with FITC, such that all parasites stained with FITC but only those that were within permeabilized host cells also stained with Texas red and thus appear yellow. (a) The effect of A23187 on the membrane integrity of host cells infected with Iie^+ (RHΔ and MBD2.1) and Iie^- (MBE1.1 and MBE3.3) strains. Cells infected with RHΔ and MBD2.1 are permeabilized despite the absence of parasite motility. This permeabilization is not observed in cells infected with MBE1.1 and MBE3.3. (b) The A23187-induced permeabilization by the Iie^+ RHΔ strain is inhibited by pretreating the infected monolayer with BAPTA-AM.

in Iie^+ strains at 2 min; data not shown), there appeared to be a 2- to 4-min delay in the timing of ^{51}Cr release in both cytochalasin D-treated and -untreated cells. This lag is probably due to sequestration of the label within host compartments (e.g., Golgi and mitochondria). The two Iie^- mutants, but not MBD2.1, showed a dramatic delay in chromium release, regardless of the presence of cytochalasin D (Fig. 8a and b). The difference in the membrane-permeabilization response to A23187 in each of the strains appears to correlate with the observed Iie phenotypes and is dependent on changes in $[Ca^{2+}]$ because the effect is blocked in all strains by BAPTA-AM pretreatment (Fig. 8c). Cells infected with the Iie^- mutant MBE1.1 do eventually get permeabilized, even in the presence of cytochalasin D, at about the time when they

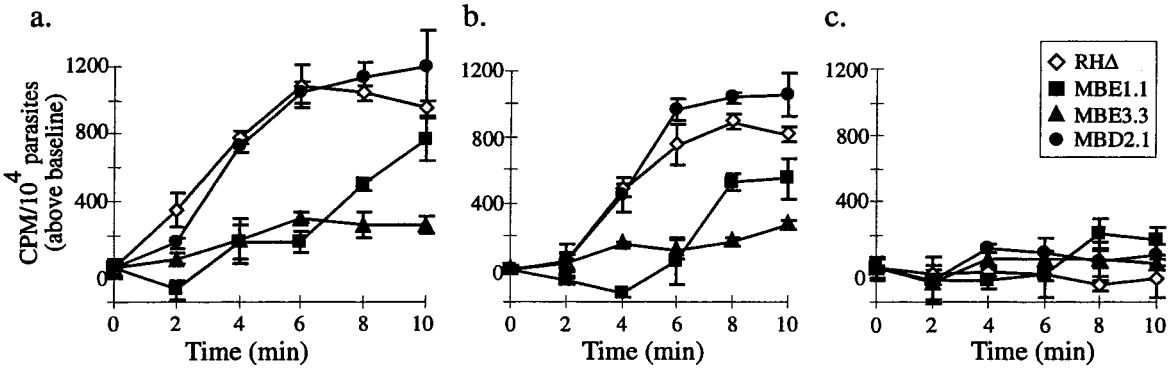

FIG. 8. Quantitation of egress-independent host lysis using a ^{51}Cr release assay. HFF monolayers were infected with either RHΔ, MBE1.1, MBE3.3, or MBD2.1 and were loaded with ^{51}Cr. Cells were pretreated with either DMSO (a), cytochalasin D (b), or BAPTA-AM (c). A23187 was then added to all cultures, and the counts per minute (CPM) obtained from ^{51}Cr release was measured and normalized to 10^4 parasitophorous vacuoles.

would usually undergo egress (Fig. 8b). This result suggests that permeabilization is a delayed but still important aspect of egress in this mutant.

Detergent permeabilization of infected host cells induces egress in a Ca^{2+}-dependent manner. The close correlation between permeabilization of the host membranes and parasite egress suggests that this process may be instrumental in IIE. To test this, the effect of host cell permeabilization on parasite egress was examined outside the context of IIE by using 0.005% saponin for 20 min at 4°C. Under these conditions, the detergent selectively permeabilizes the host cell while leaving the *Toxoplasma* membrane intact (4). After saponin permeabilization, the cells were tested for parasite egress. Under these conditions, in Ca^{2+}-containing medium host cells that were infected with the parental strain or the Iie^- mutants (MBE1.1 and MBE3.3) underwent parasite egress at similar rates (Fig. 9a). This result indicates that in the Iie^- strains, the defect in the IIE pathway is prior to permeabilization. Although we have not tested directly for the integrity of the parasite membranes after exposure to saponin, the fact that the parasites are motile and infectious immediately after the treatment suggests that they themselves have not been substantially permeabilized, as previously reported (4).

The role of $[Ca^{2+}]$ in this saponin-induced egress was examined by permeabilizing the cells in medium containing 5 mM EGTA and no added Ca^{2+} ($HBSS_{nc}$). The saponin-induced egress was dramatically inhibited for both the parental and mutant strains (Fig. 9a). Thus, there is a requirement for extraparasitic Ca^{2+} in order for the saponin permeabilization to induce egress. To test the influence of $[Ca^{2+}]$ in IIE, infected monolayers were incubated as above but using 1 μM A23187 instead of saponin to induce egress. As shown in Fig. 9b, the parental strain was fully able to undergo IIE with and without extracellular Ca^{2+}, whereas the Iie^- mutants were unresponsive to the ionophore, as previously observed. Since the ionophore is equally effective in medium containing or lacking Ca^{2+}, it is likely that the Iie^+ parasites were responding to intracellular fluxes (within the host cell and/or parasite) rather than to an influx of $[Ca^{2+}]$ from the extracellular milieu.

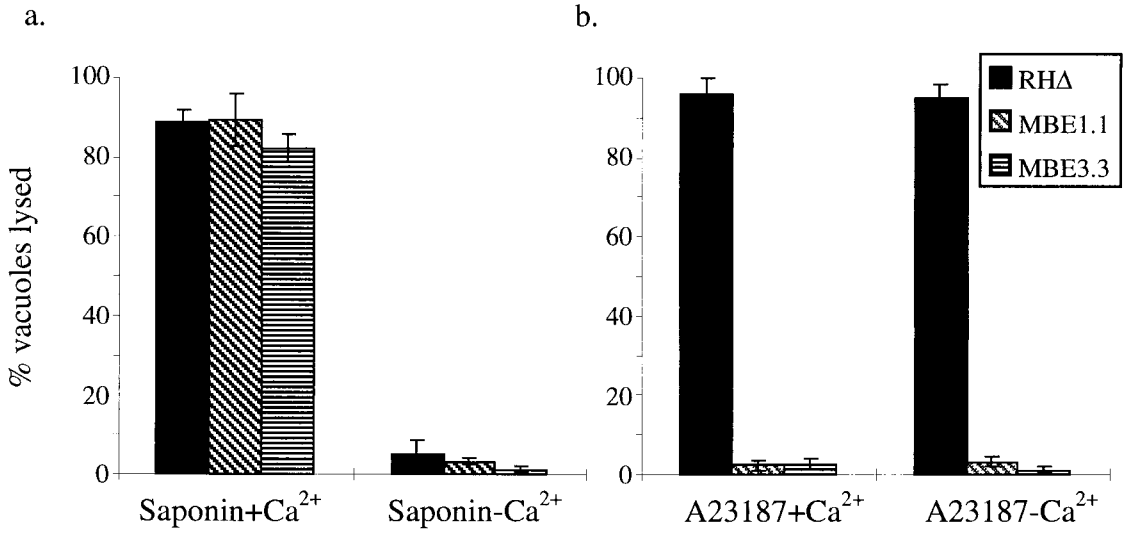

FIG. 9. Saponin induces egress in a Ca^{2+}-dependent manner. Intracellular parasites were induced to exit by treatment with either 0.005% saponin (a) or 1 μM A23187 (b) at 4°C for 20 min. After an additional 2 min of incubation at 37°C, the cells were fixed and stained. The influence of extraparasitic $[Ca^{2+}]$ on each treatment was examined by using either $HBSS_c$ (1 mM Ca^{2+}) or $HBSS_{nc}$ (5 mM EGTA and no added Ca^{2+}).

DISCUSSION

In the study reported here, several mutants of *T. gondii* resistant to the effects of the ionophore A23187 were isolated and characterized to examine the signaling pathway that induces parasite egress. Based on their resistance to IIE and IID, these mutants fall into three classes: Iie^- Iid^-, Iie^- Iid^+, and Iie^+ Iid^-. The fact that selection for Iie^- often yielded mutants that were also Iid^- (and vice versa) strongly suggests that a single mutation can give rise to both phenotypes. It is not possible to say whether these mutations involve gain or loss of function until the affected gene is identified. (Several attempts to rescue the mutants and identify the gene have thus far failed.) Likewise, it is possible that different mutations in the same gene can give rise to all three classes of mutants, but with pathways as complex as those being studied here, it is more likely that mutations in different genes are involved in each class of mutant.

A variety of assays were performed to characterize the phenotypes of representatives of the three mutant classes, and the results are summarized in Table 1. Although these mutants were isolated on the basis of defects in processes induced artificially by the use of an ionophore, all of the three Iie^- mutants have a reduced ability to productively infect host cells. Regardless of the selection scheme utilized, mutant strains showing a defect in IIE have a substantially reduced EOP. These results suggest a genetic and thus mechanistic connection between IIE and early events in the normal lytic cycle of the parasite. Another important association is that the Iie^- mutants failed to permeabilize the host cells upon exposure to A23187 in a Ca^{2+}-dependent, egress-independent manner. The importance of this step in the egress event was demonstrated by showing that the Iie^- mutants would respond to mild saponin permeabilization of the host plasma membrane and undergo egress with wild-type kinetics. This strongly suggests that the defect in the two Iie^- mutants is upstream of the permeabilization event.

Based on our results, we propose a stepwise model for the process of IIE. The first step is a rise in the $[Ca^{2+}]$ surrounding and perhaps within the parasite as a result of the ionophore releasing intracellular stores and allowing extracellular Ca^{2+} to flow in. Note that the parasitophorous vacuole is surrounded by tightly apposed host mitochondria and endoplasmic reticulum, compartments that are major stores of intracellular Ca^{2+}. The importance of Ca^{2+} outside the parasite is demonstrated by the fact that BAPTA-AM treatment of the infected host cell prior to application of the ionophore blocks conoid protrusion, gross permeabilization of the host plasma membrane, and egress. Although BAPTA-AM should not be able to enter the parasite, it is possible that minute amounts do enter and that the critical change in Ca^{2+} level is inside the parasite.

The second step in the model is parasite-dependent permeabilization of the host plasma membrane and parasitophorous vacuole. This allows a final egress signal to reach the parasites and causes them to leave the infected cell as the third and final step. The observation that polyvalent cations, such as Ca^{2+}, Mg^{2+}, Ni^{2+}, and Gd^{3+}, will induce an intracellular Ca^{2+} flux in *Toxoplasma* (22) suggests that a cation sensor on the surface of the parasite may be involved in some aspect of the IIE response.

The defect in mutant MBE1.1 can be further delimited to downstream of receipt of the initial Ca^{2+} signal since the intracellular parasites do respond to the ionophore by protruding the conoid. Thus, this mutant may receive the signal, protrude the conoid, and release its microneme contents but have a defect in the permeabilization activity normally contained within this secreted material. It is possible that the release of this permeabilization activity is detrimental to extracellular parasites, which would explain the IID seen with wild-type parasites and the resistance to it by MBE1.1. Although the mixing experiments indicate that the activity responsible for IID is not a stable, freely diffusible toxic substance, these experiments do not preclude the secretion of a toxic factor that acts only locally or transiently. It is not known whether treatment of intracellular parasites with ionophore reduces their viability. Our test for egress scored for ruptured cells, while the IID experiments looked at the infectivity of the treated parasites. If IID is caused by a local-acting secreted factor, it is possible that the intracellular parasites abandon the vacuoles before they can be affected by it. IID could also be the consequence of activation of apoptotic pathways or other lytic factors. Whether the factors ultimately causing extracellular death and intracellular host cell permeabilization are the same remains to be elucidated, but some commonality between these two phenotypes is strongly suggested by the genetic data presented here.

For MBE3.3, the block in IIE also appears to be at the permeabilization step, except in this case the conoid is not protruded and thus the defect could be due to a failure to sense the Ca^{2+} flux. Alternatively, since conoid protrusion has been associated with the release of micronemal contents (3), this mutant might contain the permeabilization activity but be unable to secrete it in response to ionophore. Extracellular MBE3.3 parasites exposed to the ionophore do protrude the conoid and release their contents, possibly because the Ca^{2+} signal received is far stronger under these conditions than when intracellular. This hypothesis is supported by the observation that elevated concentrations of A23187 did increase the efficiency of IIE in this strain (Fig. 1b) whereas MBE1.1 remained essentially unresponsive at even 20 μM. Nonetheless, the fact that extracellular MBE3.3 protrudes its conoid and dies when treated with ionophore is consistent with the notion that this mutant possesses a fully functional permeabilization activity and that, as for wild-type parasites, this could be locally toxic when released.

For the third class of mutants (Iie^+ Iid^-) represented by MBD2.1, there is no block in IIE, suggesting that the permeabilization activity is at least partially functional and released in response to the usual signals. MBD2.1 shows an increased sensitivity to BAPTA-mediated chelation of intracellular Ca^{2+} in extracellular parasites. Although the full significance of this phenotype is unknown, it does indicate that MBD2.1 has an altered capacity to respond to Ca^{2+}. This result and the fact that no significant difference in the speed or magnitude of ionophore-induced calcium flux of the mutant was seen using Indo 1AM (Sigma) (data not shown) suggest that the mutant might have a different capacity to mitigate the calcium flux but that it has no defect in its ability to take up the ionophore. Thus, the mutant might have a decreased response to intracellular $[Ca^{2+}]$ levels; that is, if intracellular $[Ca^{2+}]$ drops because of the BAPTA-AM, it loses viability but if an ionophore is applied, the rise in $[Ca^{2+}]$ is inadequate to fatally stimulate the parasites.

Saponin-induced egress for all of the mutants and for the wild type was dependent on the presence of Ca^{2+}. Because EGTA would diffuse into the permeabilized host cell, it is not possible to say if the critical lack of Ca^{2+} is in the host cytosol or the extracellular milieu. The fact that even the Iie^- mutants show the dependence on Ca^{2+} suggests that high levels of Ca^{2+} can overcome their defects and elicit the egress signal. Indeed, it is possible that the permeabilization causes a rise in $[Ca^{2+}]$ to a level far higher than is achieved by the ionophore

alone and that this is the critical egress signal proposed in the model.

In summary, these results indicate that there is a strong linkage between the different effects of Ca^{2+} ionophores and that the induction of egress involves a multistep pathway that includes permeabilization of the host cell just prior to the actual egress event. Identification of the genes that are affected in the mutants will help elucidate these pathways. Molecular genetics in this system has advanced dramatically in recent years, but complementation of phenotypes other than ones involving known biosynthetic pathways has not been reported. Efforts to recover the mutated genes in the Iie^{-} and Iid^{-} mutants have likewise not yet been successful, but as further tools are developed, this should become possible.

ACKNOWLEDGMENTS

This work was supported in part by the National Institutes of Health (AI21423, AI07328, and AI45057), the University of California AIDS Research Program, and a Predoctoral Fellowship from the Howard Hughes Medical Institute (to M.B.).

The following reagent was obtained through the AIDS Research and Reference Program, Division of AIDS, NIAID, NIH, from David Roos: *T. gondii* host strain RH(EP)ΔHXGPRT. We thank Vern Carruthers and David Sibley for the provision of the MIC2 monoclonal antibody 6D10 and help with the A23187-induced microneme secretion assay. We also thank Joe Schwartzman, Lloyd Kasper, and Elijah Stommel for assistance with characterizing the mutants and members of the Boothroyd laboratory and Chris Lekutis and Barbara Burleigh for critical reading of this manuscript.

REFERENCES

1. **Ausubel, F. M., R. Brent, R. E. Kingston, D. D. Moore, J. G. Seidman, J. A. Smith, and K. Struhl (ed.).** 1995. Current protocols in molecular biology, vol. 1. J. Wiley and Sons, Inc., Boston, Mass.
2. **Burg, J. L., D. Perelman, L. H. Kasper, P. L. Ware, and J. C. Boothroyd.** 1988. Molecular analysis of the gene encoding the major surface antigen of *Toxoplasma gondii*. J. Immunol. **141:**3584–3591.
3. **Carruthers, V. B., and L. D. Sibley.** 1999. Mobilization of intracellular calcium stimulates microneme discharge in *Toxoplasma gondii*. Mol. Microbiol. **31:**421–428.
4. **Carruthers, V. B., and L. D. Sibley.** 1997. Sequential protein secretion from three distinct organelles of *Toxoplasma gondii* accompanies invasion of human fibroblasts. Eur. J. Cell Biol. **73:**114–123.
5. **Chiappino, M. L., B. A. Nichols, and G. R. O'Connor.** 1984. Scanning electron microscopy of *Toxoplasma gondii*: parasite torsion and host-cell responses during invasion. J. Protozool. **31:**288–292.
6. **Clapham, D. E.** 1995. Calcium signaling. Cell **80:**259–268.
7. **Dobrowolski, J. M., and L. D. Sibley.** 1996. *Toxoplasma* invasion of mammalian cells is powered by the actin cytoskeleton of the parasite. Cell **84:**933–939.
8. **Donald, R. G., and D. S. Roos.** 1995. Insertional mutagenesis and marker rescue in a protozoan parasite: cloning of the uracil phosphoribosyltransferase locus from *Toxoplasma gondii*. Proc. Natl. Acad. Sci. USA **92:**5749–5753.
9. **Endo, T., K. K. Sethi, and G. Piekarski.** 1982. *Toxoplasma gondii*: calcium ionophore A23187-mediated exit of trophozoites from infected murine macrophages. Exp. Parasitol. **53:**179–188.
10. **Endo, T., and K. Yagita.** 1990. Effect of extracellular ions on motility and cell entry in *Toxoplasma gondii*. J. Protozool. **37:**133–138.
11. **Hupe, D. J., E. R. Pfefferkorn, N. D. Behrens, and K. Peters.** 1991. L-651,582 inhibition of intracellular parasitic protozoal growth correlates with host-cell directed effects. J. Pharmacol. Exp. Ther. **156:**462–467.
12. **Mondragon, R., and E. Frixione.** 1996. Ca^{2+}-dependence of conoid extrusion in *Toxoplasma gondii* tachyzoites. J. Eukaryot. Microbiol. **43:**120–127.
13. **Mondragon, R., I. Meza, and E. Frixione.** 1994. Divalent cation and ATP dependent motility of *Toxoplasma gondii* tachyzoites after mild treatment with trypsin. J. Eukaryot. Microbiol. **41:**330–337.
14. **Moreno, S. N. J., and L. Zhong.** 1996. Acidocalcisomes in *Toxoplasma gondii* tachyzoites. Biochem. J. **313:**655–659.
15. **Nicotera, P., B. Zhivotovsky, and S. Orrenius.** 1994. Nuclear calcium transport and the role of calcium in apoptosis. Cell Calcium **16:**279–288.
16. **Pezzella, N., A. Bouchot, A. Bonhomme, L. Pingret, C. Klein, H. Burlet, G. Balossier, P. Bonhomme, and J. M. Pinon.** 1997. Involvement of calcium and calmodulin in *Toxoplasma gondii* tachyzoite invasion. Eur. J. Cell Biol. **74:**92–101.
17. **Pfefferkorn, E. R.** 1977. *Toxoplasma gondii*: the enzymic defect of a mutant resistant to 5-fluorodeoxyuridine. Exp. Parasitol. **44:**26–35.
18. **Pfefferkorn, E. R., and S. E. Borotz.** 1994. *Toxoplasma gondii*: characterization of a mutant resistant to 6-thioxanthine. Exp. Parasitol. **79:**374–382.
19. **Pingret, L., J. M. Millot, S. Sharonov, A. Bonhomme, M. Manfait, and J. M. Pinon.** 1996. Relationship between intracellular free calcium concentrations and the intracellular development of *Toxoplasma gondii*. J. Histochem. Cytochem. **44:**1123–1129.
20. **Roos, D. S., R. G. K. Donald, N. S. Morrissette, and A. L. C. Moulton.** 1995. Molecular tools for genetic dissection of the protozoan parasite *Toxoplasma gondii*. Methods Cell Biol. **45:**28–63.
21. **Ryning, F. W., and J. S. Remington.** 1978. Effect of cytochalasin D on *Toxoplasma gondii* cell entry. Infect. Immun. **20:**739–743.
22. **Schwab, J. C.** 1997. Extracellular-calcium-sensing by *Toxoplasma gondii*. *In* Molecular parasitology meeting. Marine Biological Laboratory, Woods Hole, Mass.
23. **Schwab, J. C., C. J. M. Beckers, and K. A. Joiner.** 1994. The parasitophorous vacuole membrane surrounding intracellular *Toxoplasma gondii* functions as a molecular sieve. Proc. Natl. Acad. Sci. USA **91:**509–513.
24. **Seeber, F., and J. C. Boothroyd.** 1995. *E. coli* β-galactosidase as an *in vitro* and *in vivo* reporter enzyme and stable transfection marker in the intracellular protozoan parasite *Toxoplasma gondii*. Gene **22:**39–45.
25. **Sibley, L. D., S. Håkansson, and V. B. Carruthers.** 1998. Gliding motility: an efficient mechanism for cell penetration. Curr. Biol. **8:**R12–R14.
26. **Soldati, D., and J. C. Boothroyd.** 1993. Transient transfection and expression in the obligate intracellular parasite *Toxoplasma gondii*. Science **260:**349–352.
27. **Stommel, E. W., H. E. Kenneth, J. D. Schwartzman, and L. H. Kasper.** 1997. *Toxoplasma gondii*: dithiol induced Ca^{2+} flux causes egress of parasites from the parasitophorous vacuole. Exp. Parasitol. **87:**88–97.
28. **Sultan, A. A., V. Thathy, U. Frevert, K. J. H. Robson, A. Crisanti, V. Nussenzweig, R. Nussenzweig, and R. Ménard.** 1997. TRAP is necessary for gliding motility and infectivity of *Plasmodium berghei*. Cell **90:**511–522.
29. **Wan, K. L., V. B. Carruthers, L. D. Sibley, and J. W. Ajioka.** 1997. Molecular characterization of an expressed sequence tag locus of *Toxoplasma gondii* encoding the micronemal protein MIC2. Mol. Biochem. Parasitol. **84:**203–214.
30. **Wong, S. Y., and J. S. Remington.** 1993. Biology of *Toxoplasma gondii*. AIDS **7:**299–316.